Control of the breathing mechanism of a cracked rotor by using electro-magnetic actuator: numerical study

Tobias Morais, V. Jr Steffen, Jarir Mahfoud

CONTROL OF THE BREATHING MECHANISM OF A CRACKED ROTOR BY USING ELECTRO-MAGNETIC ACTUATOR: NUMERICAL STUDY

Tobias Souza Morais[(1)], Valder Steffen Jr[(1)], Jarir Mahfoud[(2)]

[(1)] Federal University of Uberlândia, School of Mechanical Engineering, Campus Santa Mônica, 38400-902, Uberlândia - MG, Brazil.

[(2)] Université de Lyon, CNRS, INSA-Lyon, LaMCoS UMR5259, F-69621, France, 69621 Villeurbanne Cedex, France.

Abstract: This paper presents a numerical study devoted to the evaluation of the possibility of monitoring and controlling the dynamic behavior of a rotating machine with a cracked shaft by using an Electro-Magnetic Actuator (EMA). The EMA is located at the mid-span of the rotor to provide active control. The opening and closure (breathing) of the crack is determined by the stress field over its cross section resulting from the dynamic bending moment. The system is nonlinear due to the fact that the crack parameters must be determined for each time step and the EMA introduces forces that are inversely proportional to the square of the gap value between the stator and the rotor. The model developed takes into account the behavior of the crack and the influence of the EMA. Simulations were carried out to access the possibility of controlling the breathing mechanism. The results obtained demonstrate the possibility of using the EMA in order to keep the crack closed along the rotation of the rotor, thus forming a self-healing scheme for the cracked rotor.

Keywords: Rotordynamics, electro-magnetic actuator, cracked rotors, breathing mechanism, crack control.

1 INTRODUCTION

The propagation of fatigue cracks may lead to catastrophic failures in rotating machines. Significant research effort has being developed over the last twenty years aiming at detecting cracks. More recently, in the context of structural health monitoring and maintenance, the safe operation of cracked shafts is desired. Then, the machine can work continuously for the longest possible time, before any intervention for repair. The crack closure phenomenon is an important variable in fatigue crack propagation and has been extensively studied through different methods [1, 2, 3]. Usually, in industrial applications the cracked shafts can be kept under operation for many years, if correctly monitored and operated before being replaced. In general, when a cracked rotor operates under the load of its own weight, the crack will open and close once per revolution forming the so-called breathing mechanism. This phenomenon makes the stiffness matrix of the shaft nonlinear and periodically time varying. In [4] the authors described a number of difficulties associated to crack identification in shafts supported by active-magnetic bearings. Quoting these authors, "it is impossible to use the traditional method with the 2X and 3X revolution super-harmonic frequency components in the super-critical speed region to detect the crack". In [5] the authors reported having accomplished the active health monitoring of rotor-dynamics systems in the presence of cracked shafts performing the breathing phenomenon. In the two latter references the crack model used did not consider the breathing behavior of the crack as a function of the dynamical behavior of the structure, but only as a function of the rotor angular position. The breathing model was introduced to describe the crack behavior in [6], i.e., the cross coupled stiffness in a simple crack model with its parameters depending on the sign of the localized coordinate in the crack position was considered. The abrupt opening and closure of the crack as explained in this reference cannot completely

express the real breathing mechanism. Applied fracture mechanics concepts considering a localized flexibility due to cracks, resulting in a complete local flexibility matrix of a cracked shaft, were studied in [7, 8]. An experimental validation for the breathing behavior considering a shaft instrumented with many strain gages around the crack position was presented in [9]. Thus, it was possible to verify the stiffness variation along the shaft rotation and to validate the results by using a crack model. A method through which it is possible to determine the time varying stiffness due to the crack by using a time-domain orthogonal function methodology was developed in [10].

In the present paper, the crack model depends on the dynamic bending moment that acts in the ends of the cracked element. As the fatigue process in rotating shafts is characterized by the breathing mechanism, this paper proposes an approach that permits keeping the system operating by slowing down the progress of the fatigue process. This is achieved by using an Electro-Magnetic Actuator (EMA), which controls the dynamics of the system so that the total opening of the crack is avoided. To meet this requirement four actuators are arranged along two perpendicular directions, which apply attraction forces that produce bending moments to maintain the crack closed. The electro-magnetic actuator is used to compose a self-healing system in such a way that the rotor can continue its operation since the increase of the fatigue crack is avoided. The present contribution is focused on the modeling and simulation of rotating systems with two nonlinear sources: *i*) a crack that produces variation in the stiffness as a function of the stress field over the shaft cross section that depends on the crack's angular position, and *ii*) the control forces applied by the EMA that depend on the shaft displacement. For this aim three sub-systems are modeled and described in the following: the rotor, the crack, and the actuator.

The present contribution is devoted to applications related to steady state rotating conditions. The possibility of interfering on the breathing mechanism of the crack may lead to a new possible use of active magnetic bearings.

2 ROTOR MODEL

The dynamic response of the considered mechanical system can be modeled by using the Hamilton's principle. For this aim, the strain energy of the shaft and the kinetic energies of the discs and shaft are calculated. An extension of Hamilton's principle makes possible to include the effect of energy dissipation. The parameters of the bearings are included in the model by using the principle of the virtual work. For computation purposes, the finite element method (FEM) is used to model the structure so that the energies calculated are concentrated at the nodal points. Shape functions are used to connect the nodal points. To obtain the stiffness of the shaft the Timoshenko's beam theory was used and the cross sectional area was updated as proposed in [11]. The model obtained is represented mathematically by a set of differential equations as given by Equation (1):

$$\mathbf{M}\ddot{\boldsymbol{x}}(\boldsymbol{t}) + \left[\mathbf{C_b} + \dot{\emptyset}\mathbf{C_g}\right]\dot{\boldsymbol{x}}(\boldsymbol{t}) + \left[\mathbf{K(t)} + \ddot{\emptyset}\mathbf{K_g}\right]\boldsymbol{x}(\boldsymbol{t}) = \boldsymbol{F_u}(\boldsymbol{t}) + \boldsymbol{F_{EMA}}(\boldsymbol{t}) \quad (1)$$

where: $\boldsymbol{x}(\boldsymbol{t})$ is the generalized displacement vector; $\mathbf{M}$, $\mathbf{C_b}$, $\mathbf{C_g}$ and $\mathbf{K_g}$ are the well known matrices of inertia, bearing viscous damping, gyroscopic effect with respect to the rotation velocity ($\dot{\emptyset}$) and gyroscopic effect with respect to the acceleration of the rotation ($\ddot{\emptyset}$), respectively [12]. $\mathbf{K(t)}$ is the stiffness matrix for the system containing the cracked element, and $\boldsymbol{F_u}(\boldsymbol{t})$ and $\boldsymbol{F_{EMA}}(\boldsymbol{t})$ are forces due to unbalance and Electro-Magnetic Actuator (EMA), respectively.

The system studied is presented in Figure 1. It is composed of a horizontal flexible shaft of 0.04 m of diameter and two discs represented by D_1 and D_2. The shaft is supported by symmetric bearings at its ends: two ball bearings at the left hand end (2. 10^8 N/m stiffness and 800 N.s/m viscous damping) and a roller bearing at the right hand end (1.10^6 N/m and 800 N.s/m). The EMA is represented by B_2. Its position is chosen by considering the dynamic behavior of the system (efficiency of the electro-magnetic actuator on the dynamics of the crack).

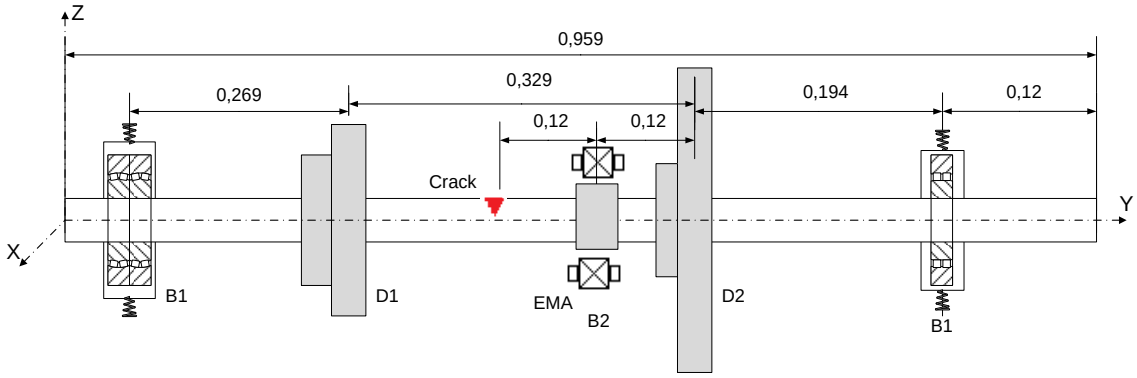

Figure 1. Rotor System.

A finite element model shown in Figure 2 was used to carry out the numerical simulations. For this aim, the model contains the following elements: rigid discs with only kinetic energy contribution, flexible shaft with kinetic and strain energies as represented by Timoshenko beam elements with two nodes per element and 4 degrees of freedom (d.o.f.) per node. Only the displacement response generated by using the first eight modes at the EMA position was considered for all analyses performed.

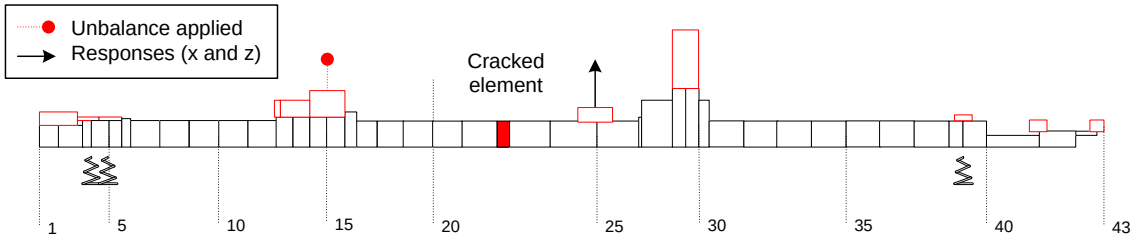

Figure 2. Rotor Finite Element Model.

The simulation was performed by using a computer code that was built on the MATLAB/SIMULINK® environment. The optimization tools used in the present study were already previously developed as in [13].

3 CRACK MODEL

The breathing mechanism is a result of the stress and strain distribution around the cracked area, which is due to static loads (such as the rotor weight), the bearing reaction forces, and the dynamic loads (such as the unbalance and the vibration induced by the inertia force distribution). When the static loads overcome the dynamic ones, the breathing is governed by the angular position of the shaft with respect to the stationary load direction, so that the crack opens and closes completely once at each revolution. The transition from closed crack (full stiffness) to open crack (residual stiffness) has been generally considered as being abrupt [6] or represented by a given cosine function. The corresponding calculation can be carried out step by step through an iterative procedure as proposed in this paper.

The opening and the closing (breathing) of the crack is determined by the stress field over its cross section as caused by the dynamic bending moments. The hypothesis of heavy rotor, for which the dynamic behavior of the crack (opening and closing) is only a function of the rotor angular position, is discarded in the present contribution. Here, the

system is nonlinear and the crack parameters have to be determined for each time step. The model of the breathing mechanism used in this paper is based on reference [9].

The breathing mechanism calculation is summarized in the flowchart shown in Figure 3. The identification process starts with the estimation of the crack parameters and the modeling of the structure through the finite element method. It is considered that the crack influences only the stiffness parameters. Consequently, it is assumed that the other parameters do not change in the presence of a crack. For determining the stiffness matrix of the cracked element, $K_c(t)$, it is necessary to calculate first the second moments of inertia of the cross section where the crack is located. For this aim, the cross section is meshed as shown in Figure 4. Then, the geometric center and the moments with respect to this point are obtained. The opening and closing of the crack are given as a function of the stress field resulting from the dynamic efforts and weight of the structure.

The tensile stress should be calculated for each element of the meshed cross section, Figure 4. If the stress field along the crack is positive, it means that the region is under traction, i.e., the crack is opened and does not contribute to the calculation of the moments of inertia. Consequently, a reduction is observed in the values of the elements of the stiffness matrix. On the other hand, if the field along the crack is negative, the region is under compression, i.e., the crack is considered closed thus contributing to the moments of inertia of the cross section and to the corresponding stiffness elements of the stiffness matrix.

Due to the cross section asymmetry, the tensile stress is given by:

$$\sigma = \frac{M_z I_{xx} + M_x I_{xz}}{I_{xx} I_{zz} - I_{xz}^2} x - \frac{M_x I_{zz} + M_z I_{xz}}{I_{xx} I_{zz} - I_{xz}^2} z \qquad (2)$$

The dynamic moments M_x and M_z are given from the strength of materials theory: $\frac{\partial \theta_x}{\partial y} = \frac{M_x}{EI}$ and $\frac{\partial \theta_z}{\partial y} = \frac{M_z}{EI}$ where θ_x and θ_z are the rotations with respect to the axes x and z, respectively. In practice, $\partial \theta_x = \theta_x^{i+1} - \theta_x^i$ is considered, where i is the node at the end of cracked element and $\partial y = L_c$, where L_c is the length of this element, as illustrated in Figure 5.

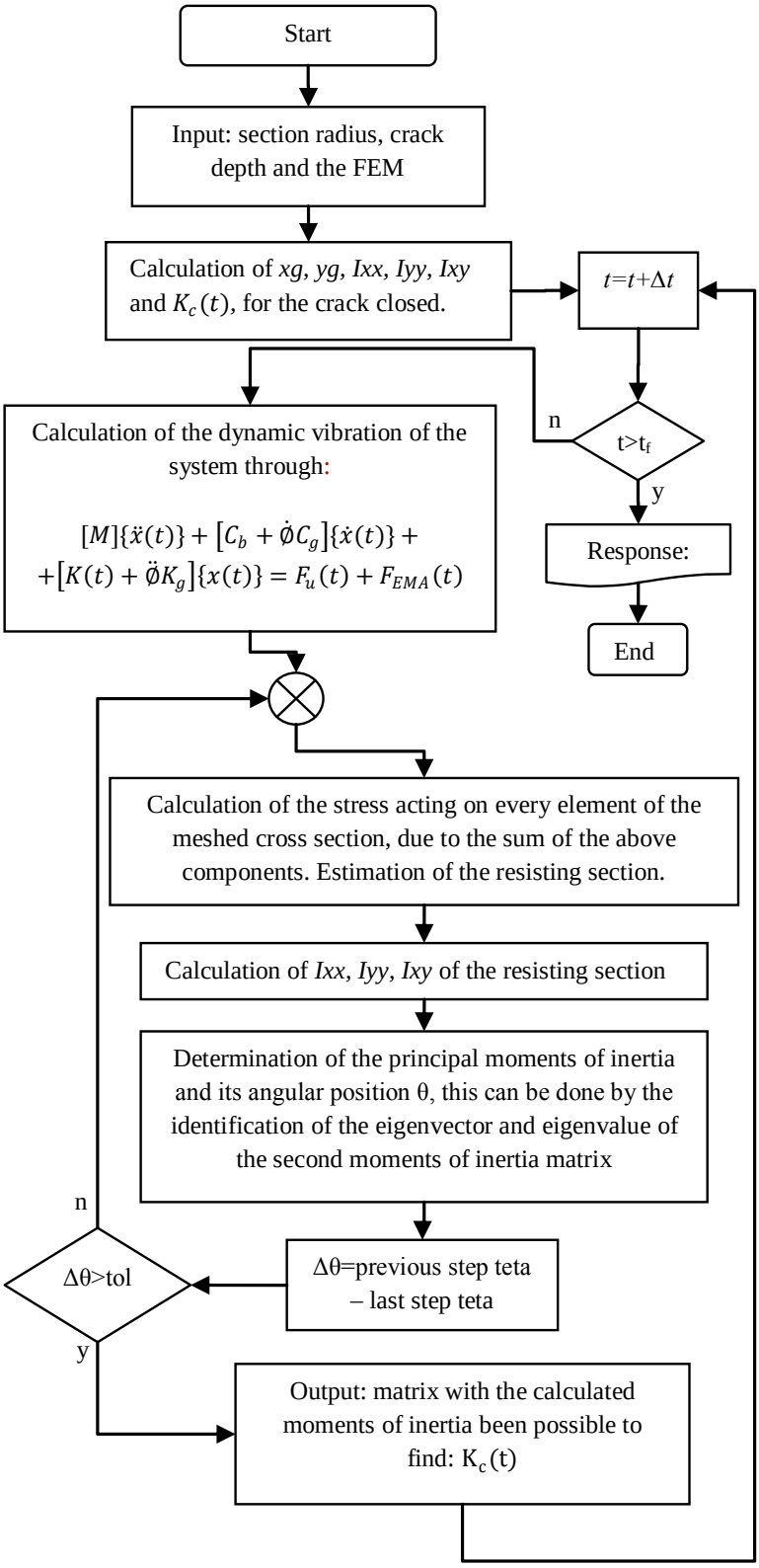

Figure 3. Flowchart for the iterative calculation of the breathing mechanism with the EMA.

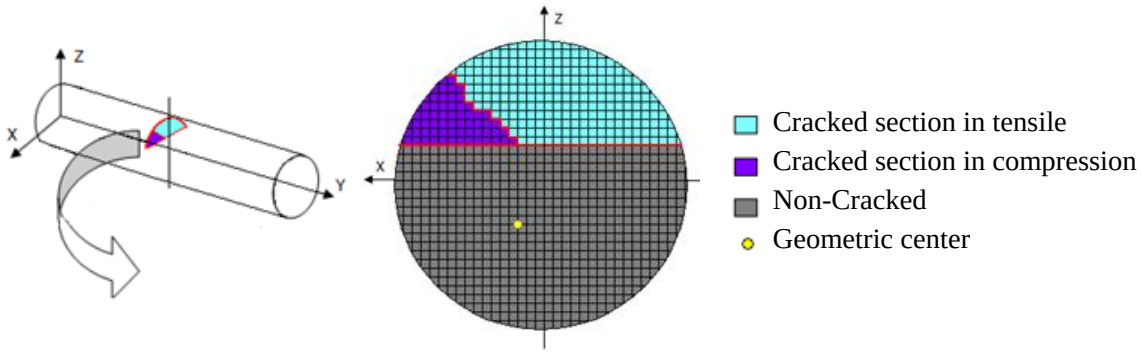

Figure 4. Cross section of the cracked element.

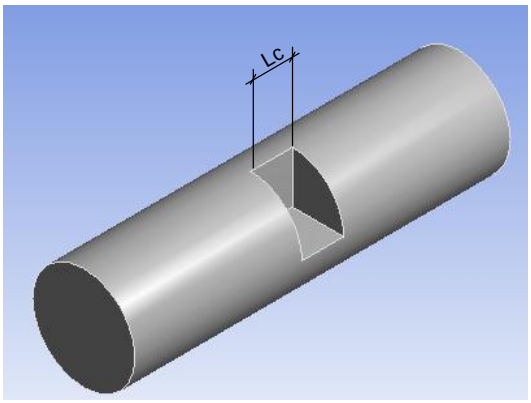

Figure 5. Equivalent cracked beam element.

Once the breathing mechanism and the area moments of inertia have been defined, as previously described, the stiffness matrix of an equivalent cracked beam element of suitable length, L_c, can be calculated by assuming a Timoshenko's beam theory. Constant cross section and constant area moments of area along the length of the element are considered, as shown in Figure 5. The neighboring beam elements are simply uniform circular cross section beams. This model is considered a simplified flexible model.

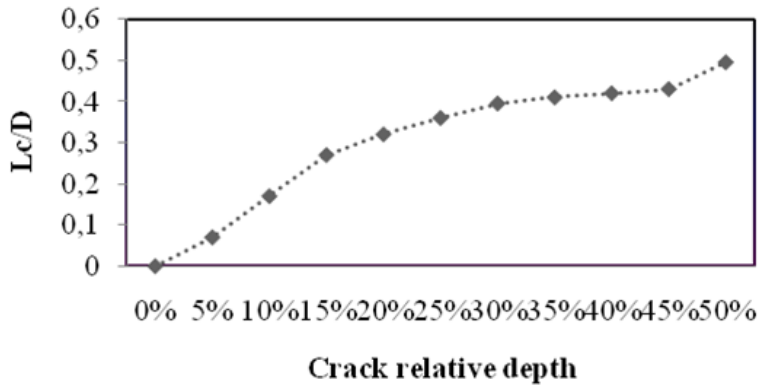

Figure 6. Relationship between the crack relative depth p, the diameter D and the length L_c of "equivalent" beam.

It is possible to obtain a three-dimensional model that derives from the nonlinear finite element technique. In Figure 6 a relation involving both the simplified flexible model and the 3D model is presented. This relation permits the determination of the optimal length value of the cracked element that is used to fit the simplified model to the 3D model.

The stiffness matrix (square 8×8 symmetrical matrix) is represented by equation (3). More details regarding the identification of this matrix can be found in [4].

$$\mathbf{K_c(t)} = \begin{bmatrix} b & p & -q & -d & -b & -p & -q & -d \\ p & a & c & q & -p & -a & c & q \\ -q & c & e & r & q & -c & f & s \\ -d & q & r & h & d & -q & s & g \\ -b & -p & q & d & b & p & q & d \\ -p & -a & -c & -q & p & a & -c & -q \\ -q & c & f & s & q & -c & e & r \\ -d & q & s & g & d & -q & r & h \end{bmatrix} \begin{Bmatrix} x_i \\ z_i \\ \theta_{x\,i} \\ \theta_{z\,i} \\ x_{i+1} \\ z_{i+1} \\ \theta_{x\,i+1} \\ \theta_{z\,i+1} \end{Bmatrix} \quad (3)$$

where the coefficients that appear in the matrix above are defined as:

$$a = \frac{12\, I_{yy}E}{(1+\phi)L_c^3}, b = \frac{12I_{xx}E}{(1+\phi)L_c^3}, c = \frac{6I_{yy}E}{(1+\phi)L_c^2}, d = \frac{6I_{xx}E}{(1+\phi){L_c}^2},$$

$$e = \frac{(4\ +\phi)I_{yy}E}{(1+\phi)L_c}, f = \frac{(2-\ \phi)I_{yy}E}{(1+\ \phi)L_c}, g = \frac{(2-\ \phi)I_{xx}E}{(1+\ \phi)L_c}, h = \frac{(4+\phi)I_{xx}E}{(1+\phi)L_c},$$

$$p = \frac{12\, I_{xy}E}{(1+\phi)L_c^3}, q = \frac{6I_{xy}E}{(1+\phi)L_c^2}, r = \frac{(4+\phi)I_{xy}E}{(1+\ \phi)L_c}, s = \frac{(2-\ \phi)I_{xy}E}{(1+\ \phi)L_c},$$

$$\text{and } \phi = \frac{12EI}{GSL_c^2}$$

The parameter ϕ accounts for the shear effects, E and G are respectively the Young's modulus and the shear modulus, S is the cross section area, and I represents the second moments of area.

4 ACTUATOR MODEL

The Electro-Magnetic Actuator (EMA) used in this paper, Figure 7, consists of 4 electromagnetic coils; each one applies an attraction force [14] whose mathematical representation is shown in Table 1.

The forces applied by the electro-magnetic actuators ($\boldsymbol{F_{EMA}}$) are written as a function of two constants C_1 and C_2 that depend on the geometric properties of each electro-magnetic actuator. Also, these forces are a function of the air gap value (e) and the co-localized displacement (δ). The values of the coil parameters used in this work are given in Table 1. These values correspond to a real EMA that is commonly used in experimental work.

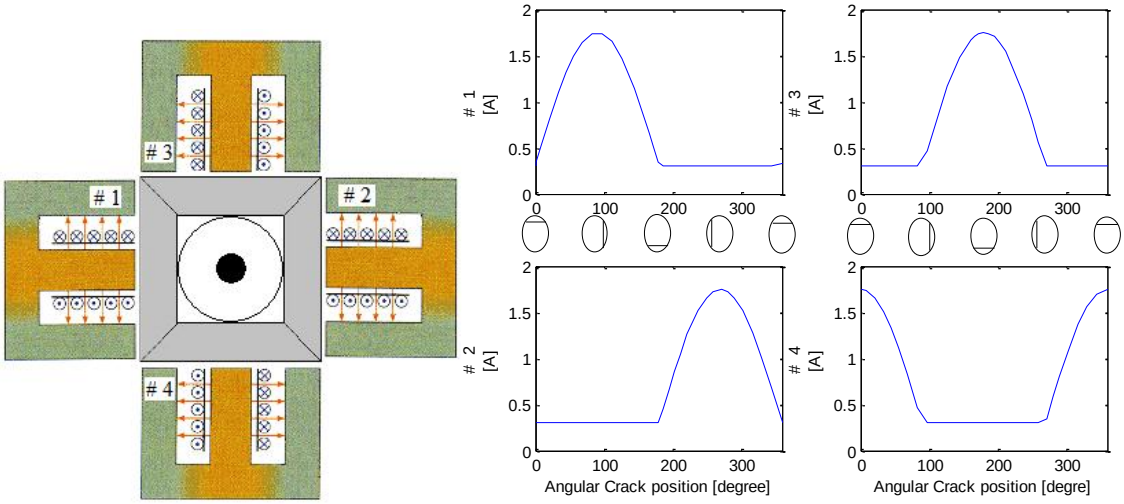

Figure 7. Electric current design for each coil as a function of the angular position of the rotor.

Table 1. Coil parameters.

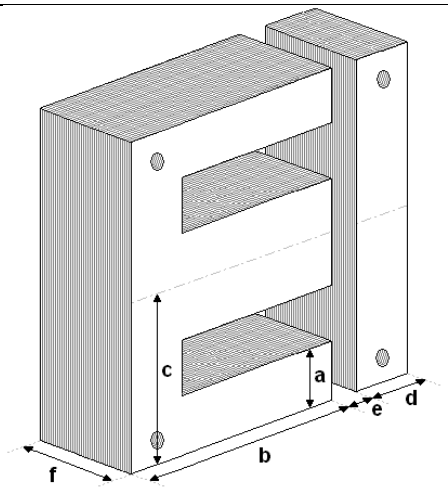

μ_0 (H/m)	1.2566E-06
μ_r (H/m)	700
N (Spires)	278
a (mm)	21
b (mm)	84
c (mm)	63
d (mm)	21
e (mm)	1.5

$$F_{em} = \frac{\mu_0 . f . a . (NI)^2}{2\left((e \pm \delta) + \frac{b + c + d - 2a}{\mu_r}\right)^2}$$

The currents used to drive the coils were designed so that they exhibit two terms, namely a constant current in each coil that is added to a varying current depending on the crack angular position. The constant form is used to contribute to vibration reduction for some speeds of rotation; however, constant currents are not necessary for other speeds of rotation in the operation range of the machine as can be seen in Figure 7. This configuration aims at producing an attraction force that is sufficiently large to avoid the total opening of the crack and small enough to avoid a significant increase of the structure displacements. The varying currents follow a sinusoidal law, which begin at the time when the point P (crack position) passes to the opposite side of the coil. These varying currents reach a maximum value when P is at the most distant position with respect to the coil and are zero when it returns to the same side of the coil, as shown in Figure 7. This result was obtained for the case in which a constant current of 0.3 A was used in each coil. For the case in which the rotor performs an inverse whirl motion the configuration of these currents is such that they keep the crack open, i.e., their feature is precisely the opposite of the previous one.

5 DESCRIPTION OF THE CRACK CLOSURE APPROACH

The procedure to minimize the crack opening can increase the vibration level of the rotor, thus leading to undesired side effects. Consequently, the goal of the proposed approach at this point is to determine a current combination that is capable of minimizing the crack opening and, at the same time, does not induce either large vibrations or instability to the system. Consequently, a multi-criteria optimization context is formulated. Various optimization techniques are available to handle the problem. In the present paper, the authors have chosen a heuristic method, the so-called Particle Swarm Optimization (PSO), to determine the optimal parameters of the system.

The choice of this method is related to its simplicity, easiness of implementation and the ability of avoiding local minima that may appear in the design space. It was developed by the social psychologist James Kennedy and the electrical engineer Russel Eberhart [15], as emerged from experiences with algorithms inspired in the social behavior of some bird species. PSO is a global optimization technique for dealing with problems in which the best solution can be represented as a point or surface in an n-dimensional space [16].

The multi-objective function takes into account simultaneously the following criteria: *i*) the reduction of the crack opening, Equation (4), and *ii*) the minimization of the system vibration, Equation (5) and Equation (6), as measured along the *x* and z directions, respectively, at the position of the EMA. The design variables considered are the following: four constant currents and four variable currents for the coils, thus totalizing eight design variables.

$$F_1 = \frac{\left(S(t) - Ar(t)\right)^2}{\left(S(t)\right)^2} \tag{4}$$

$$F_2 = \sum_{j=1}^{np} \left(x(t)_j\right)^2 \tag{5}$$

$$F_3 = \sum_{j=1}^{np} \left(z(t)_j\right)^2 \tag{6}$$

where: Ar and S are the cross section areas of the element with and without crack, respectively, and x_j and z_j are the vibration displacements along the *x* and *z* directions for each measurement point (np), respectively.

Figure 8 shows the variation of the unbalance response, during run-down from 4500 rpm to rest, for different values of the electric current for the case in which constant currents are applied to the coils. It can be observed that the vibration amplitude decreases as the current intensity increases, for determined rotation speed ranges. Also, a shift of the critical speeds is observed as the current increases. This behavior motivates the use of the constant part of the current. Besides, when the rotor is mounted horizontally the weight influences the dynamics of the crack significantly. The constant current minimizes the static deformation of the rotor. Finally, it is expected that the optimization method is able to find zero current intensity depending on the given rotation speed; also, different current intensities are supposed to be found for the rotor either in the horizontal or vertical configurations.

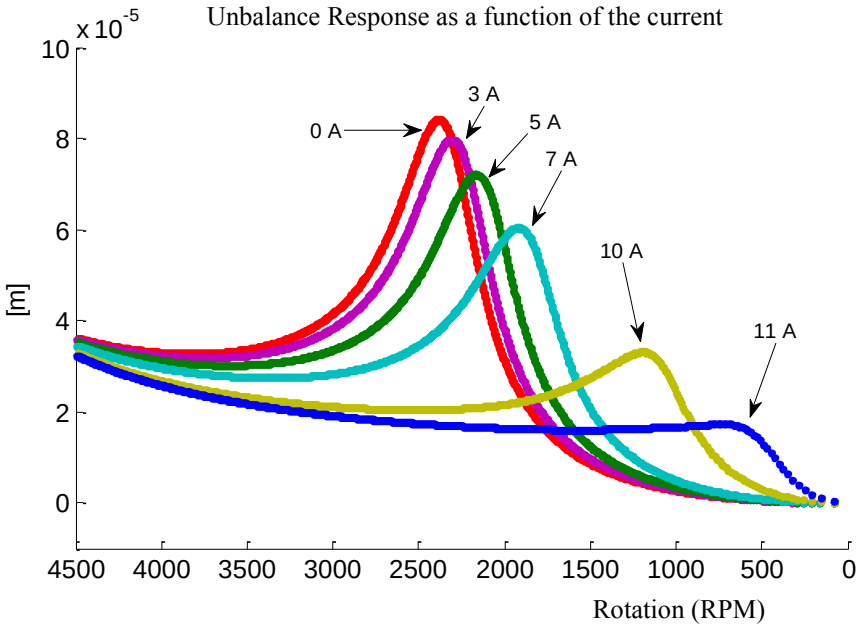

Figure 8. Unbalance Response (run-down) for a non-cracked rotor as a function of the electric current.

6 RESULTS AND DISCUSSION

Two system configurations are addressed: first, a flexible rotor was mounted in the vertical position so that the weight does not influence the crack dynamics; second, the same rotor was mounted horizontally so that the weight becomes an important factor in the dynamics of the crack. For simulation purposes, the crack depth used was equal to the shaft radius and the length of the cracked element was determined according to Figure 6. For the optimization process 120 individuals were considered and 80 iterations were performed. The currents range from 0 to 5 A, corresponding to values that are commonly found in experimental work.

6.1 Vertical Rotor

The system was simulated considering the gravity force as being equal to zero, i.e., the crack breathing is given as a function of dynamic efforts of the structure, only. An unbalance of 80 g.cm and phase 0^o was applied to disc D_1. The steady state rotation was fixed to 1500 rpm. The results found by using the optimization method are given as follows: for the continuous currents – no driving current for the 4 coils (null currents); for the varying currents - the current amplitudes are 1.80 A for the coil #1, 1.80 A for the coil #2, and 0.33 A for the coils #3 and #4. As seen in Figure 8 the continuous currents of the coils would make the vibration level increase for the rotation speed considered. This behavior confirms the result given above for these currents (as they are all zero). These results were found for a sampling time of 1 second and the EMA was turned off after 0.7 sec.

The responses calculated at the EMA position are shown along the *x* and *z* directions, respectively as shown in Figure 9. The variation of the area moments of inertia as a function of time is depicted in Figure 10. The variation of the cross sectional area varies

similarly. It can be seen that the crack is kept almost closed (negligible variation) while the current is applied.

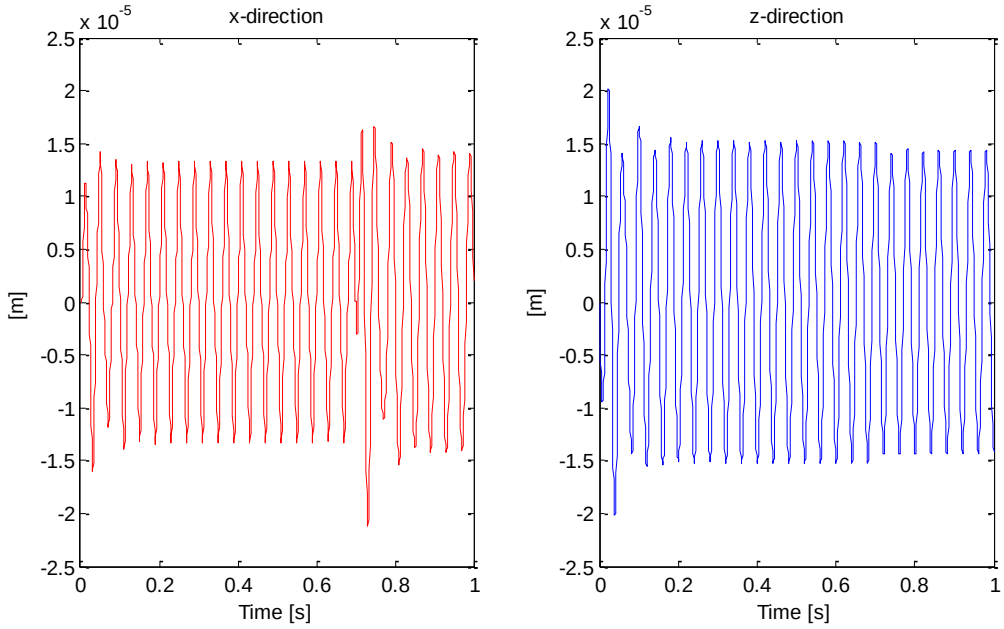

Figure 9. Response of the system calculated at the EMA position

(the electromagnetic actuator was turned off after 0.7 s).

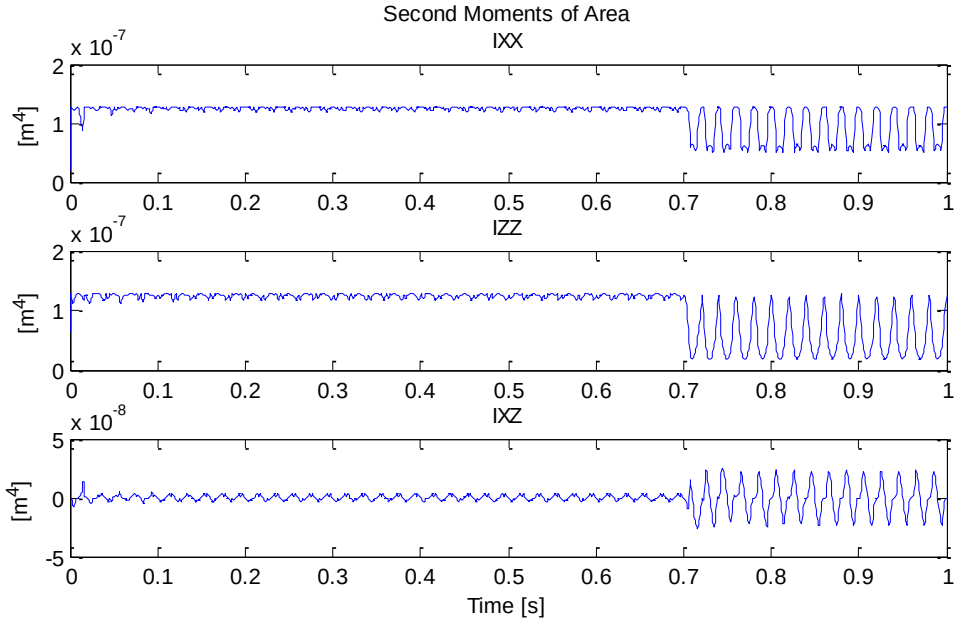

Figure 10. Area moments of inertia of the cross section.

Finally, the necessary forces have been analyzed to check if the designed actuators are able to provide these forces accordingly. The resulting forces along the *x* and *z* directions are presented in Figure 11, respectively. It is worth mentioning that for the configuration of the currents considered (see Figure 7), the electromagnetic force along the *x* direction is considerably higher than the one along the *z* direction. The corresponding currents have the same behavior. This means that the actuators mounted on a single direction (*x* or *z*) would be able to control the breathing mechanism for the rotor mounted on the vertical position.

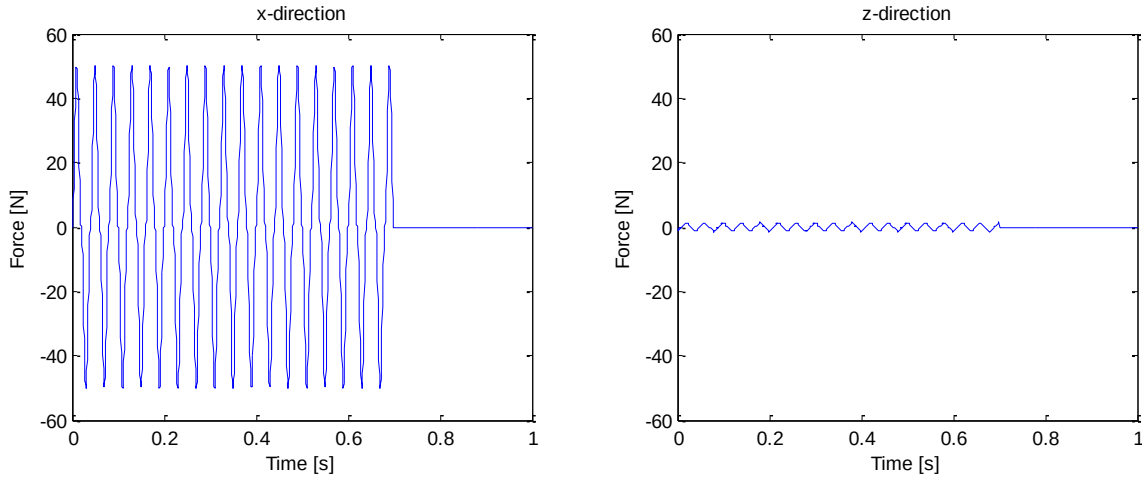

Figure 11. Control forces for the breathing mechanism.

6.2 Horizontal Rotor

In this case the crack breathing is given as a function of both the dynamic efforts and the weight of the structure. It is known that the weight itself makes the bending deformation more evident and promotes the initiation of the crack. The same unbalance and the same rotation speed as for the previous case study were considered. The results found by the optimization method for the continuous currents were zero for the coils, except for coil #3, for which it was found to be 3.11 A. For the varying currents the

following amplitude values were obtained: 2.28 A for coil #1, 2.28 A for coil #2, 0.44 A for coil #3, and 0.08 A for coil #4. Similar to the previous case, the results for the horizontal rotor are displayed along 1 second and the EMA was turned off after 0.7 sec.

In Figure 12 the time responses calculated at the EMA position are shown along the directions *x* and *z*, respectively. The displacements obtained remain at acceptable values, i.e., the additional energy introduced by the controller does not produce unaffordable displacements in the system.

The variation of the cross sectional area with respect to time is shown in Figure 13. It can be observed that the crack is kept almost closed while the actuator is working. The configuration of the rotor corresponding to the horizontal position characterizes a more difficult control environment as compared to the vertical position, due to the weight effect.

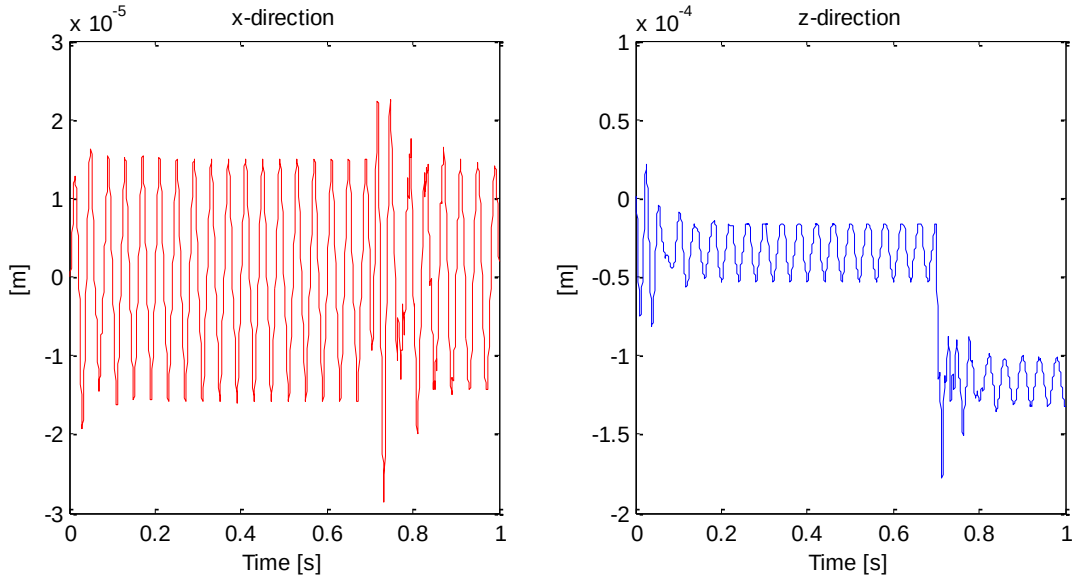

Figure 12. Response of the system calculated at the EMA position

(the electromagnetic actuator was turned off after 0.7 s).

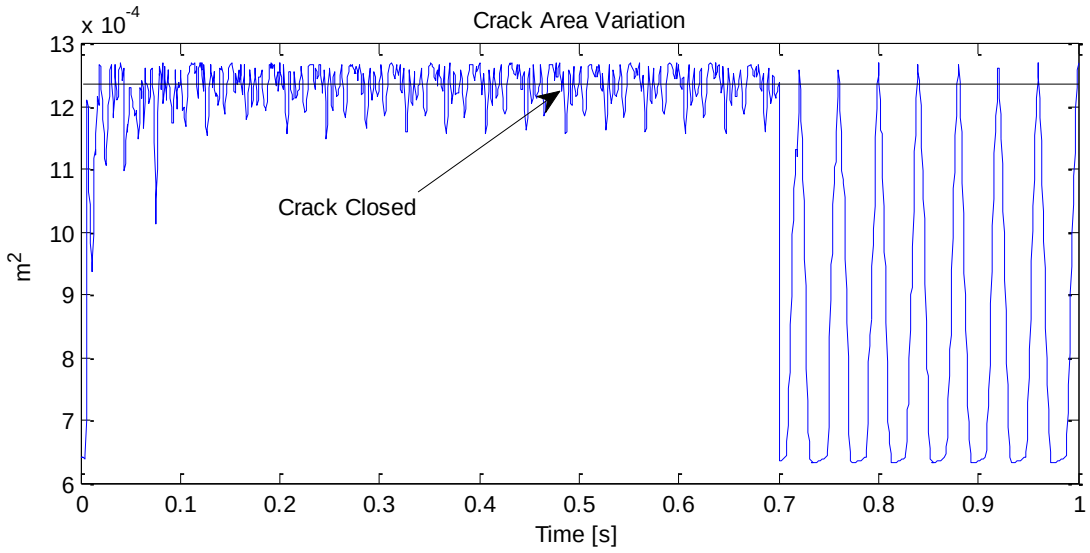

Figure 13. Cross Section of the cracked element.

As in the previous case the resulting control forces could be easily reproduced experimentally (Figure 14). Differently from the vertical rotor, the present configuration requires control forces along both directions, *x* and *z*. The resulting control force along the *z* direction corresponds approximately to the weight of the rotor.

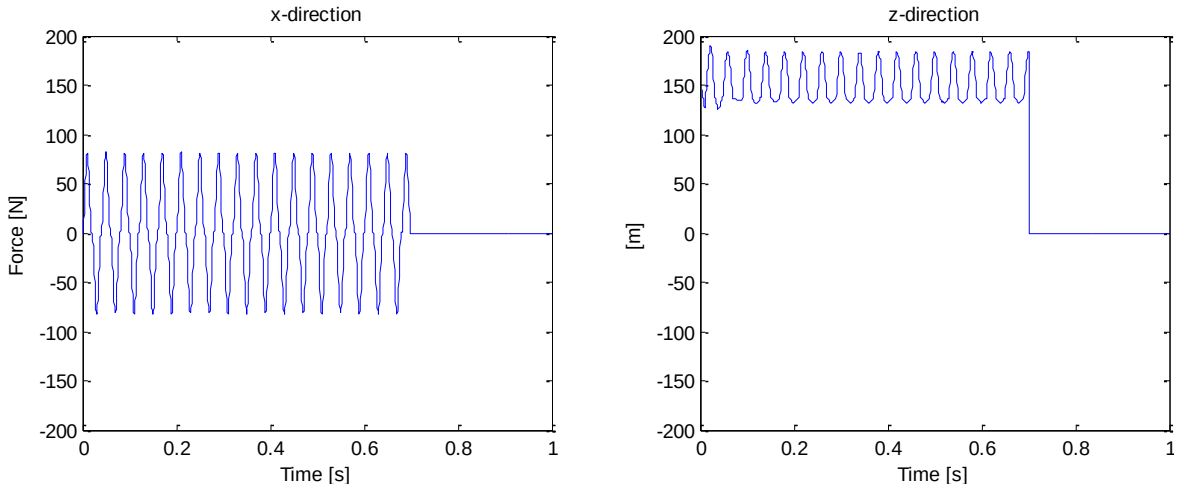

Figure 14. Control forces for the breathing mechanism control.

7 CONCLUSION

This paper demonstrated the possibility of controlling the fatigue process of a rotating machine by using electro-magnetic actuators. For the identification of the currents to drive the actuators validated models for the following sub-systems are required: flexible rotor, crack, and actuator. Otherwise, it would be necessary to measure the resistant cross section area for different time instants, which is not possible experimentally. In the case of the vertical rotor, the actuators mounted on a single direction would be able to control the breathing mechanism. Differently, the horizontal configuration requires control forces along the directions *x* and *z*. For this case, the resulting control force along the *z* direction corresponds mainly to the weight of the rotor. It is expected that the identified currents are able to keep the crack closed when applied to real systems. The amplitudes of the control forces are plausible from the experimental point of view. The presented results were obtained for a steady state condition. Next step would be to observe the transient behavior of the system by using high performance controllers.

8 ACKNOWLEDGEMENTS

The authors are thankful to the Brazilian research foundations FAPEMIG and CNPq (Proc. Nb. 574001/2008-5; INCT-EIE) for providing financial support to this work.

9 REFERENCES

[1] **Stoychev, S.** and **Kujawski, D.** Methods for Crack Opening Load and Crack Tip Shielding Determination: A Review, Fatigue & Fracture of Engineering Materials & Structures, 2003, Vol. 26, N^{o} 11, pp. 1053-1067.

[2] **Nowell, D.** Techniques for Experimental Measurement of Fatigue Crack Closure, Applied Mechanics and Materials, 2007, Vol. 7-8, pp. 3-9.

[3] **Pu, Y., Chen, J., Zou, J.** and **Zhong, P.** The Research on Non-Linear Characteristics of a Cracked Rotor and reconstruction of the Crack Forces, Journal of Mechanical Engineering Science, 2002, Vol. 216, N^{o} 11, pp. 1099–1108.

[4] **Changsheng, Z., Robb, D. A.** and **Ewins, D. J.** The Dynamic of a Cracked Rotor with an Active Magnetic Bearing, Journal of Sound and Vibration, 2003, Vol. 265, N^{o} 3, pp. 469–487.

[5] **Mani. G., Quinn, D. D.** and **Kasarda, M.** Active Health Monitoring in a Rotating Cracked Shaft Using Active Magnetic Bearings as Force Actuators, Journal of Sound and Vibration, 2006, Vol. 294, N^{o} 3, pp. 454-465.

[6] **Gasch, R.** A Survey of the Dynamic Behaviour of a Simple Rotating Shaft with a Transverse Crack, Journal of Sound and Vibration, 1993, Vol. 160, N^{o} 2, pp. 313-332.

[7] **Dimaragonas, A. D.** and **Papadopoulos, C. A.** Vibration of Cracked Shafts in Bending, Journal of Sound and Vibration, 1983, Vol. 91, N^{o} 4, pp. 583-593.

[8] **Papadopoulos C. A.** and **Dimaragonas A. D.** Coupled Longitudinal and Bending Vibration of a Rotating Shaft with an Open Crack, Journal of Sound and Vibration, 1987, Vol. 117, N^{o} 1, pp. 81-93.

[9] **Bachschmid, N., Pennacchi, P., Tanzi, E.** and **Audebert, S.** Transverse Crack Modeling and Validation in Rotor Systems, Including Thermal Effects, International Journal of Rotating Machinery, 2003, Vol. 9, N^{o} 2, pp. 113-126.

[10] **Morais, T. S., Steffen Jr, V.** and **Bachschmid, N.** Time-Varying Parameter Identification Using Orthogonal Functions, Journal of Physics: Conference Series, 2008, Vol. 135, N^{o} 1, pp. 012072.

[11] **Hutchinson, J. R.** Shear Coefficients for Timoshenko Beam Theory, Journal of Applied Mechanics, 2001, Vol. 68, No 1, pp.87-92.

[12] **Lalanne, M.** and **Ferraris, G.** Rotordynamics Prediction in Engineering, Second Edition, John Wiley and Sons, 1998.

[13] **Viana, F. A. C.** Surrogate Modeling Techniques and Heuristic Optimization Methods Applied to Design and Identification Problems, PhD Thesis, Federal University of Uberlândia, Uberlândia, Minas Gerais, Brazil, 2008.

[14] **Der Hagopian, J.** and **Mahfoud, J.** Electromagnetic Actuator Design for the Control of Light Structures, Smart Structures and Systems, 2010, Vol. 6, N^o 1, pp. 29-38.

[15] **Kennedy, J.** and **Eberhart, R. C.** Particle Swarm Optimization, IEEE International Conference on Neural Networks, Perth, Australia, 1995, Vol. 4, pp. 1942–1948.

[16] **Pomeroy, P.** An Introduction to Particle Swarm Optimization, 2003, Available in http://www.adaptiveview.com/articles/ipsoprnt.html.

NOMENCLATURE

$\boldsymbol{x(t)}$ is the generalized displacement vector;

$\mathbf{M}$ is the matrix of inertia;

$\mathbf{C_b}$ is bearing viscous damping matrix;

$\mathbf{C_g}$ is the matrix of the gyroscopic effect with respect to the rotation velocity;

$\mathbf{K_g}$ is the matrix of the gyroscopic effect with respect to the acceleration of the rotor;

$\dot{\emptyset}$ is the angular velocity;

$\mathbf{K(t)}$ is the stiffness matrix for the system containing the cracked element;

$\boldsymbol{F_u(t)}$ is the unbalance force vector;

$\boldsymbol{F_{EMA}(t)}$ is the force vector related with the Electro-Magnetic Actuator (EMA);

M_x is the dynamic moment with respect with the *x*-axis;

M_z is the dynamic moment with respect with the *z*-axis;

I is the second moment of area of the element;

E is the Young's Modulus;

G is the Shear Modulus;

θ_x is the rotation with respect to the *x*-axis;

θ_z is the rotation with respect to the *z*-axis;

L_c is the length of the cracked element;

S is the cross section area;

ϕ is the parameter that accounts for the shear effects;

C_1 and C_2 are constants that depend on the geometric properties of each electro-magnetic actuator;

e is the air gap value.;

δ is the co-localized displacement;

P is the crack position;

Ar is the cross section area of the cracked element;

x_j and z_j are the vibration displacements along the *x* and *z* directions, respectively;

np is the number of measures;

t is the time vector.